

PLENARY LECTURES

PL1

40+ Years of NMR: Now and Then

Sunney Chan

Institute of Chemistry, Academia Sinica

Abstract: In this lecture, I will recall the developments of NMR over the past 50 years, as perceived through the eyes of a romantic “nomad” who happened to have wandered into the field by random walk some 40 years ago. Even at age 50 plus, NMR continues to amaze me as a vibrant intellectual discipline with many exciting possibilities for applications across a broad front of science. The power and limitation of NMR for some of these applications will be highlighted and discussed.

40+ Years of NMR

Now & Then

PL2

Dynamics and Function of Enzymes

H. Jane Dyson

Department of Molecular Biology, The Scripps Research Institute, 10550 North Torrey Pines Road, La Jolla CA 92037.

Abstract: Molecular motions are widely regarded as contributing factors in many aspects of protein function. NMR studies of polypeptide chain dynamics in the function of two enzymes provide examples of the wide variety of roles that molecular motions can play in enzyme function. An NMR study of the metallo- β -lactamase from *Bacteroides fragilis* shows the importance of motion in mediating the wide substrate specificity of this important antibiotic-resistance enzyme. The enzyme dihydrofolate reductase (DHFR), and particularly that from *Escherichia coli*, has become an important system for investigating the linkage between protein dynamics and catalytic function, both because of the location and timescales of the motions observed and because of the availability of a large amount of structural and mechanistic data that provides a detailed context within which the motions can be interpreted. Changes in protein dynamics in response to ligand binding, conformational change, and mutagenesis have been probed using numerous experimental and theoretical approaches, including X-ray crystallography, fluorescence, nuclear magnetic resonance (NMR), molecular dynamics simulations, and hybrid quantum/classical dynamics methods. These studies provide a detailed map of changes in conformation and dynamics throughout the catalytic cycle of DHFR and give new insights into the role of protein motions in the catalytic activity of this enzyme.

PL3

Quantitating Protein Folding Thermodynamics and Dynamics using NMR shifts and Linewidths

Niels H. Andersen,* Bipasha Barua, Stephanie A. Endsley, R. Matthew Fesinmeyer, F. Michael Hudson, Jasper C. Lin, and Katherine A. Olsen

Department of Chemistry, University of Washington, Seattle, WA 98195, U.S.A.

Abstract: Short peptide sequences that have definable, stable conformations in aqueous media and display protein-like folding behavior serve as excellent systems for determining the structural requirements of protein folds and for optimizing folding rates and pathways. These small (8- to 26-residue) systems have short fold lifetimes (typically less than 20 μ sec), which makes NMR a particularly powerful tool for assessing folding cooperativity. In this time regime, chemical shifts are population-weighted averages, allowing the calculation of the folding equilibrium constant, while linewidths still reflect inter-state transition rates. Complete folding cooperativity requires that all structuring shifts decrease at the same rate in a melt or chemical denaturation. NMR-monitored melting studies can also provide the temperature dependence of ΔG_U and the extent and nature of residual structuring (if any) in the unfolded ensemble. Such studies provide unique insights into the effects of mutations in miniproteins and β -sheet models and can be used to guide the mutational optimization of fold stability and/or folding rates. Examples will be drawn from our current studies of β -hairpins, three-stranded sheet models (including WW domain mimics), $\beta\beta\alpha$ domains, and Trp-cage miniproteins. Representative sequences of stabilized and destabilized Trp-cages and a series of β hairpins appear below. The β hairpins can be viewed as optimized and minimized versions of the second hairpin of the B1 domain of protein G (GB1p) and the trpzip system of Cochran.

| | | |
|-----------------------|-----------------------------------|----------------------------------|
| Optimized Trp-cage | DAYAQWLKDG GPSSGRPPPS | $T_m = 61^\circ\text{C}$ |
| a destabilized form | DAYAQWLKDG GPSSGRPA PS | $T_m = 39^\circ\text{C}$ |
| cage disruption | DAYAQWLKDG GPSSGRPPAS | 20% folded at 7°C |
| GB1p | GEW TY DDATK TFTVTE | $T_m < 7^\circ\text{C}$ |
| GB1m3 (stable analog) | KK WTY NPATGK FTYQE | $T_m = 62^\circ\text{C}$ |
| Trpzip equivalent | KK WTW NPATGK WTWQE | $T_m = 85^\circ\text{C}$ |
| minimized | KTW NPATGK WTE | $T_m = 68^\circ\text{C}$ |
| further minimized | AWS NGK WT | $T_m = 24^\circ\text{C}$ |
| NPATGK turn | AcNPATGK-NH ₂ | < 8% folded at 7°C |

The basis for the high propensity of the NPATGK loop to support hairpin formation was defined by further NMR studies. Even though this loop can form a stabilized H-bonded turn, hairpin formation absolutely requires cross-strand hydrophobic interactions and the turn is poorly populated in the absence of these hydrophobic interactions. The hairpin folding process is essentially two-state.

Both the hairpin and cage models display unusually large ring current shifts (2 – 3.6 ppm). Under fast and intermediate exchange regimes, the line broadening associated with unfolding transitions depends on $(\delta_F - \delta_U)^2$. As a result, all of these systems display exchange broadening even though folding times, $(k_F)^{-1}$, are in the 0.5 – 40 μsec range and the effects of temperature and mutations on folding and unfolding rates (over the 5 – 60 $^\circ\text{C}$ range in water) can be extracted from very simple NMR experiments. For example, while both the optimized trp-cage and GB1m3 display $(k_F)^{-1} = 1\text{-}2.5 \mu\text{sec}$ at 298K; for WT GB1p, $(k_F)^{-1} = 23 \mu\text{sec}$ under the same conditions. Other mutational and solvent effects on folding rates will be presented.

[Supported by grants from the U.S. National Institutes of Health (GM59658) and NSF
(CHE0315361)]

PL4

Field-Cycling NMR in a Shared Commercial Spectrometer: Applications to Nucleic Acids, Proteins, and especially Membranes (and lots more!)

A.G. Redfield

Brandeis University, and Mary F. Roberts, Boston College.

Abstract: Our apparatus wheels into the small 500 NMR (Varian) room, and pokes a precision glass shuttle tube into the top hole of the magnet. The sample is raised and lowered by air pressure/vacuum and the round trip time is 0.2 to 0.4 sec. (1). It is relatively simple and can in principle be adapted to any NMR instrument. In Toronto we presented 2D ^{15}N relaxation results (with D. Kern and E. Eisenmesser) that confirm expected relaxation behavior in Cyclophilin A down to 3 T, below which the rate is too fast for us to measure (unpublished). We also presented ^{31}P T_1 data on a DNA octamer duplex, which provides a clean separation of CSA relaxation at high field, and dipolar relaxation from protons below about 2T. The CSA showed a definite increase in rate at high field (up to 16 T) due to high-frequency motion, which could be approximately reproduced by a simulation (2). Our ^{31}P relaxation data in phospholipid vesicles from 50 G to 11.7 T shows dynamic behavior with three time-scales: A very low-field relaxation dispersion with a microsec scale corresponding to overall head-to tail diffusion of a lipid molecule due to viscous tumbling of the vesicle (4); a 5 nanosec dispersion that we attribute to rotational diffusion of the lipid about the membrane perpendicular (the director) (3); and CSA relaxation at high field (>3T) similar to what we saw in the DNA sample (3). From the dipolar relaxation rates at the two field we get the angle between the director and the diester phosphate-to-C3 protons, distances, and other information. I will describe these experiments and mention others for which this simple device could be used.

- 1.A. Redfield (2003) *Magn.Reson. in Chem* **41**:753-768;
- 2.A. Redfield, Q. Cui, C. J. Turner, D. A. Case, & M. F. Rogers (2004) *Biochemistry* **43**: 3637-3650;
- 3.A. G. Redfield and M. F. Roberts (2004) *J. Amer. Chem. Soc.* (in press);
- 4.A. G. Redfield and M. F. Roberts (2004) *Proc. Nat. Acad. Sci. USA* (in press).

Supported by NIH Grant GM60418 (M. F. R.) and PRF/ACS Grant 36680-AC4 (AGR)

PL5

Stereo-Array Isotope-Labeling (SAIL) Method -High-throughput and Accurate Structural Determinations of Proteins

Masatsune Kainosho

CREST of JST and Graduate School of Science, Tokyo Metropolitan University

Abstract: Structural determinations of proteins by NMR spectroscopy have so far been limited to those smaller than 25 kDa. Much effort has been exerted to extend this molecular size limits, but utilize uniformly ^{13}C and/or ^{15}N labeled samples. However, the molecular size limits of the proteins to be studied remain ~ 30 kDa and structural determinations of proteins around this size-limit still remain quite challenging, if possible. This is where deuterium labeling can play a major role again. Methods such as random fractional deuteration or selective protonation, which have already been exploited, are compromises and extend the molecular size limit at the expense of signal sensitivity and the accuracy of the resultant structure. More robust and uncompromised techniques should therefore be developed, if NMR spectroscopy is to remain to be a competitive method for structural determinations of larger proteins and protein complexes. During the 40 year history of biological NMR spectroscopy, it has been clear that concomitant advances in spectroscopic methods and in preparative methods of isotopically labeled proteins are essential to overcome the numerous difficulties. Here we propose an innovative new strategy named stereo-array isotope-labeling (SAIL) and present some of the recent results obtained using this strategy.

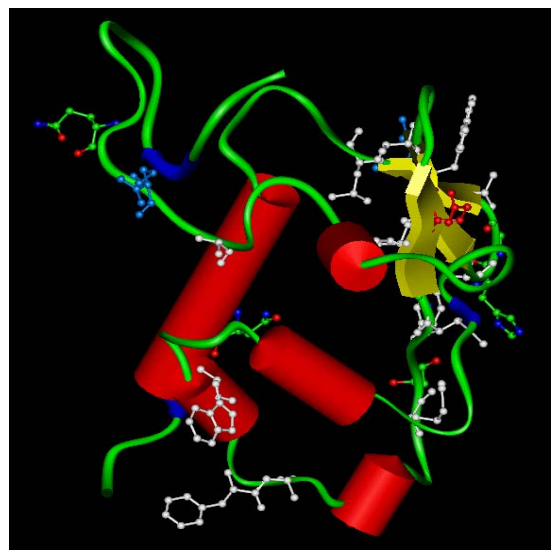
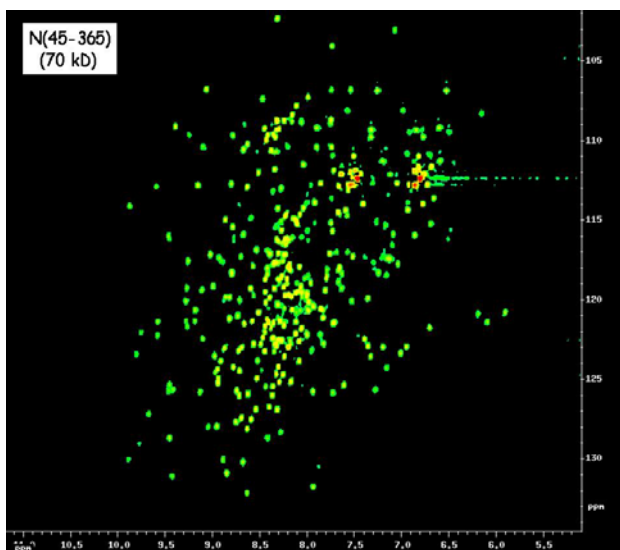
PL6

The Structure of SARS-Associated Coronavirus Nucleocapsid (N) Protein

Chung-ke Chang¹, Shih-che Su¹, Chen-kun Tsai^{1,2}, Chiu-min Hsieh¹, Tsan-hung Yu¹, Yan-jie Jiang³, Shin-jye Lee^{1,&}, Hsiao-yi Hung³, Hsin-hao Hsiao¹, Wen-jin Wu¹, **Tai-huang Huang**^{1,2}

¹*Institute of Biomedical Sciences, Academia Sinica;* ²*Department of Physics, National Taiwan Normal University;* ³*Department of Agronomy, National Taiwan University, Taipei, Taiwan, ROC*

Abstract: The SARS-CoV N protein is a 423 amino-acid protein that shares little sequence homology with other members of the coronavirus family. It is a major antigen in severe acute respiratory syndrome and is presumed to bind with the RNA genome to form a helical core within the viral envelope. The SARS-CoV N protein has also been suggested to involve in other important functions in viral life cycle. In order to gain deeper insight into structure-functional relationship we have undertaken the task of determining the structure of the SARS-CoV N protein. We showed that the N protein consists of two independent structural domains, the RNA binding domain (RBD) (a.a. 45-181) and the dimerization domain (OGD) (a.a. 248-365). The remainder of the sequence appears to be disordered. We further showed that the C-terminal structural domain is responsible for N protein dimerization. The structure of OGD consists of five α -helices and a three-strand anti-parallel β -sheet. A β -sheet region has also been identified as the primary hydrophobic interface. Our results provide a framework for understanding the structure-function relationship of SARS coronavirus nucleocapsid protein and provide new insights on its mechanism of function at the molecular level.



INVITED LECTURES

L1

How glycosphingolipid move amphiphilic polypeptide to form membrane pores

Wen-Guey Wu

Institute of Bioinformatics and Structural Biology, National Tsing Hua University, Hsinchu, 30043, Taiwan

Abstract: Cobra cardiotoxin (CTX), a cytotoxic beta-sheet basic polypeptide, is well known to cause membrane leakage in many cells including human erythrocytes, cardiomyocytes and smooth muscle cells. We have also shown recently in model and biological membrane studies that CTX-induced membrane pore formation exhibits specificities toward sulfatide-containing membranes. In this talk, by reviewing recent works on (1) NMR structure of sphingolipids in membranes, (2) NMR structure of sulfated carbohydrate complexed to CTX, (3) lipid binding site of CTX revealed by NMR and (4) X-ray crystal structures of CTX-sulfatide complex in membrane-like environment at 2.3Å resolution, we propose a molecular mechanism at atomic resolution to explain the role of sulfoglycosphingolipid in promoting CTX membrane pore formation. The model indicates an important role of lipid conformation at the membrane interface to promote insertion of amphiphilic polypeptide into lipid bilayers. It is suggested that lipid headgroup conformational change from a bent to a fully extended orientation near the membrane surface may serve as a general mechanism to allow lipid move polypeptides from a peripheral into a penetration binding mode.

L2

Functional-Structural Studies of DNA-binding Proteins from Thermoacidophilic Archaea *Sulfolobus*

Andrew H.-J. Wang

Institute of Biological Chemistry, Academia Sinica

Abstract: The archaeobacteria *Sulfolobus solfataricus* and *S. acidocaldarius*, are hyperthermophilic and acidophilic organisms which live in sulfur-rich hot springs at greater than >80 °C and pH 2~3. How does DNA maintain its chemical and physical integrity in those organisms is an interesting question. In eukaryotic cells, the genomic DNA is packed by histones into nucleosomes, which in turn form higher-order structures of chromatin. The structural organization of DNA in prokaryotes and archaeobacteria is somewhat less well understood. In this paper we studied the structural-functional relation of several low molecular weight DNA-binding proteins, including Sso7d/Sac7d, Sso10b2 and Sso7c4. They all bind DNA without marked sequence preference and increase the T_m of DNA significantly.

The crystal structures of several Sac7d/Sso7d-DNA complexes have revealed an unexpected DNA binding mode in which a sharp kink in DNA was observed. The observations suggest the role of those proteins in the packing of DNA to organize chromatin structures in these archaea, which lack histones, and offer insights into the possible role of several classes of the minor groove DNA-binding proteins. Sac7d/Sso7d used Val26 and Met29 hydrophobic amino acids on a β -sheet for intercalation to DNA, causing a 60° single-step kink. We investigate the interaction and binding property of different Sac7d Val26 and Met29 mutants with DNA. These two hydrophobic side chains were systematically changed to either smaller or larger sizes. Our results will help understand the molecular basis of protein-induced DNA kinks. New proteins may be engineered to modulate the extent of DNA curvature.

Next, by appending a leucine-zipper-like helical peptide to the C-terminal end of Sac7d, the monomers are expected to form a dimer. The formation of dimer was detected by various biochemical and biophysical methods which showed that the DNA-binding capacity was retained. X-ray crystal structure of S7dLZ in complex with decamer DNA CCTATATAGG showed that the leucine-zipper segments of S7dLZ were associated into an antiparallel four-helix bundle, and each tetramer binds two DNA fragments. This model works as a successful template that endows protein a new function without losing original properties.

Another protein, Sso10b2, is an 89aa protein which binds both DNA and RNA. The structure adopts a $\beta\alpha\beta\alpha\beta\beta$ topology, similar to Sso10b1 (also called Alba), and other RNA-binding proteins including IF3-C, YhhP and DNase I.

Finally, Sso7c proteins were originally identified as repressor-like proteins. We have cloned and expressed the protein Sso7c4. The structure of the 54aa basic protein was solved by NMR spectroscopy which revealed a triple antiparallel β -sheet capped with a short α -helix on one side. The protein forms a dimer at low concentration as analyzed by AUC. The fold of the dimer structure is akin to that of *Bacillus subtilis* transition-state regulator AbrB. The crystals of Sso7c4 have been obtained which diffract x-rays to 1.9 Å resolution.

Other DNA-binding proteins from *Sulfolobus* are currently under study.

References

1. Robinson, H., et al. (1998) *Nature* **392**, 202-205. "The Hyperthermophile Chromosomal Protein Sac7d Kinks DNA Sharply."
2. Yang, J.-M. and Wang, A. H.-J. (2004) *J. Biomol. Struct. Dyn.* **21**, 513-526 "Engineering a thermostable protein with two DNA-binding domains using the hyperthermophile protein Sac7d."
3. Ko, T.-P., et al. (2004) *Acta. Cryst.* **D60**, 1381-1387. "Crystal structures of the hyperthermophilic chromosomal protein Sac7d in complex with DNA decamers."
4. Chen, C.-Y., et al., (2005, in press) *Nucleic Acids Res.* "Probing the DNA kink structure induced by the hyperthermophilic chromosomal protein Sac7d."
5. Wu, S.-W., et al (2005, in revision) *Proteins*. "Design and characterization of a multimeric DNA binding protein using Sac7d and GCN4 as templates."

L3

Design of Potent and Selective Integrins $\alpha_{\text{IIb}}\beta_3$, $\alpha_v\beta_3$, $\alpha_5\beta_1$, and $\alpha_4\beta_1$ Antagonists

Woei-Jer Chuang* Chiu-Yueh Chen, Yi-Chun Chen, Yao-Husin Hsieh, Jia-Hau Shiu

Department of Biochemistry, National Cheng Kung University College of Medicine, 1 University Road, Tainan, Taiwan

E-mail: wjcnmr@mail.ncku.edu.tw

Abstract: Integrins are large heterodimeric cell surface receptors found in many animal species ranging from sponges to mammals. They are involved in fundamental cellular processes such as attachment, migration, proliferation, differentiation, and survival. They also contribute to the initiation and/or progression of many common diseases including neoplasia, tumor metastasis, immune dysfunction, ischemia reperfusion injury, viral infections, osteoporosis, and coagulopathies. The aim of our research is to clarify, in which diseases do integrins $\alpha_{\text{IIb}}\beta_3$, $\alpha_v\beta_3$, $\alpha_5\beta_1$, and $\alpha_4\beta_1$ play a role and how could these integrin antagonists be applied as treatments. The blockade of platelet integrin $\alpha_{\text{IIb}}\beta_3$ reduces ischemic complications when used as an adjunct to percutaneous coronary intervention or the management of acute ischemic syndromes. Integrins $\alpha_v\beta_3$ and $\alpha_5\beta_1$ are over-expressed during various stages of metastatic dissemination and, in particular, during tumor reestablishment. It is well known that integrin $\alpha_4\beta_1$ is a therapeutic target for asthma. It has been shown that the disintegrin scaffold is optimized for RGD recognition sequence in integrins $\alpha_{\text{IIb}}\beta_3$, $\alpha_v\beta_3$, and $\alpha_5\beta_1$, and for LDV recognition sequence in integrin $\alpha_4\beta_1$. Disintegrins are a family of platelet aggregation inhibitors found in snake venoms containing 47 to 84 amino acids with 4-7 disulfide bonds. They inhibit platelet aggregation by blocking the binding of fibrinogen to the integrin $\alpha_{\text{IIb}}\beta_3$ of platelets. The conserved RGD sequence in the disintegrin family plays the most important role in recognizing integrins. Rhodostomin is a potent inhibitor of platelet integrin receptor and consists of 68 amino acids including six disulfide bonds and a PRGDMP sequence at the positions of 48-53. Our previous report showed that Rho expressed in *P. pastoris* possesses the same function and structure as native protein. Using rhodostomin as the scaffold, we combined site-directed mutagenesis on rhodostomin, bioassays, NMR study, molecular modeling of integrins, rational drug design, and synthesis of peptide analogs to develop the antagonists for integrins $\alpha_{\text{IIb}}\beta_3$, $\alpha_v\beta_3$, $\alpha_5\beta_1$, and $\alpha_4\beta_1$. Our results indicated that the amino acid residues flanking the RGD motif control the width and dynamics of the RGD loop and the orientation of D residue of the RGD

motif. These results provide important structural information for the design of more potent RGD mimetics and serve as the basis for exploring the structure and functional relationships of integrins and their ligands.

L4

The Interaction of Somatostatin with Sodium Dodecyl Sulfate Micelle

Wei Jyun Chien

Department of Applied Chemistry, Chaoyang University of Technology, Wufeng, Taichung, Republic of China

Abstract: Somatostatin is a disulfide-linked 14-residue cyclic peptide (SRIF-14), which interacts with 5 types of trans-membrane receptor proteins. The conformation somatostatin has been simulated under a membrane mimic environment, a negatively charged SDS micelle, based on the constraints derived from NMR experiments. In the presence of SDS micelles, the central residues in the bioactive region (Phe7-Trp8-Lys9-Thr10) of the peptide were found to adopt either a loose-defined type II' β -turn, or a more conserved type I' β -turn. Upon binding to SDS micelles, a noticeable decrease in the amide-proton exchanging rate of the Phe7-Trp8-Lys9-Thr10 segment in somatostatin was observed. This sequence-specific effect of micelle interaction was also monitored by the homo-nuclear nonselective spin-lattice relaxation times measurement. These results, together with the paramagnetic broadening observation on peptide protons in the presence of spin-labeled lipids, formed a basis of a detailed model, proposed in this study, which described the interaction of somatostatin with the lipid surface. The Asn⁵-Phe¹¹ fragment interacted with SDS micelle, while the Phe⁶-Phe⁷-Trp⁸-Lys⁹ stayed close to the center of the micelle. The association constant of somatostatin to SDS micelle, determined via pulsed-field-gradient NMR techniques, was about $1.1 \times 10^3 \text{ M}^{-1}$. Upon replacing lysine with alanine (SRIF-14 K⁴A, SRIF14-K⁹A), all analogues exhibited similar conformation with native somatostatin on SDS surface. On the other hand, the binding constants between the peptides and micelles varied according to the following trend: SRIF14-K⁹A > SRIF-14 K⁴A > SRIF-14. In modulating the binding of somatostatin and the micelles, our observations suggested that Lys⁹ maybe more important than Lys⁴, which is consistent with the fact that the Lys⁹ replaced mutant was biologically inactive.

L5

NMR Structural Studies of African Swine Fever Virus DNA Polymerase X and Its Complexes with Gapped DNA and Mg/dNTPs

Mei-I Su¹ and Ming-Daw Tsai¹⁻⁵

*Genomics Research Center¹, Academia Sinica
Department of Chemistry² and Biochemistry³, Ohio State Biochemistry Program⁴, Campus
Chemical Instrument Center⁵, The Ohio State University*

Abstract: The African swine fever virus DNA polymerase X (Pol X) is the smallest nucleotidyl transferase identified to date. It has been characterized as the least faithful DNA polymerase, which may be involved in the mutagenic viral base excision repair (BER) pathway. The solution structure of Pol X has been solved, which consists of only palm and fingers subdomains based on ~55 % sequence homology of C-terminal half of mammalian DNA polymerase β (Pol β). The important structural features are conserved between Pol X and Pol β . However, without the thumb subdomain, which is important for DNA binding in other DNA polymerases, Pol X binds gapped DNA substrates with high affinity. The potential DNA binding site is mapped out by 2D ¹⁵N-HSQC experiments, which is located between the interface of palm and fingers subdomains as well as helices α C and α E. Furthermore, the ternary complexes of Pol X with gapped DNA substrates and four different deoxynucleotides (dNTPs) are analyzed by 2D ¹⁵N-HSQC experiments. The residues involved in discrimination of different dNTPs are located closely to the kink between helices α D and α E in the fingers subdomain and helix α B-loop-strand β 5 in the palm subdomain. Given that Pol X is also characterized to catalyze four Watson-Crick base pairs and one mismatched base pair, G:G, with similar efficiencies, NMR structural studies of the G:G mismatched ternary complex are performed. Based on the preliminary results, the modeled G:G mismatched ternary complex is calculated, which shows contacts between dGTP and residues on loop-strand β 5. This may provide structural insights into the specific binding affinity of Pol X to dGTP. Further NMR experiments are considered to solve the G:G mismatched ternary complex.

L6

Novel solution structure of porcine β -microseminoprotein

Iren Wang^{1,2}, Yuan-Chao Lou³, Kuen-Phon Wu³, Shih-Hsiung Wu^{1,2*}, Wen-Chang Chang², Chinpan Chen^{3*}

¹*Institute of Biological Chemistry, Academia Sinica, Taipei 115, Taiwan;*

²*Institute of Biochemical Sciences, National Taiwan University, Taipei 106, Taiwan;*

³*Institute of Biomedical Sciences, Academia Sinica, Taipei 115, Taiwan*

Abstract: A number of β -microseminoproteins (MSPs) have been identified from different species. MSPs are all non-glycosylated and disulfide bond-rich, but show a relatively low level of conservation. Although all Cys residues are conserved, our previous study showed that the disulfide bond pairings differ in porcine and ostrich MSPs. Despite a variety of biological functions have been suggested for MSPs, their real function is still poorly understood. Furthermore, no 3D structure has been reported for any MSP, so the determination of the structure and function of MSPs is an interesting and important task. In the present study, we determined the 3D solution structure of porcine MSP on the basis of 1018 restraints. The ensemble of 20 NMR structures was well defined, with average root mean square deviations (RMSD) of 0.83 ± 0.16 Å for the backbone atoms and 1.37 ± 0.17 Å for heavy atoms in residues 2 to 90. The 3D structure showed that porcine MSP is clearly composed of two domains, an N-terminal domain consisting of one double-stranded and one four-stranded antiparallel β -sheets, and a C-terminal domain consisting of two double-stranded antiparallel β -sheets. The orientation of the two domains was derived mainly on the basis of long-range NOEs and verified using residual dipolar coupling data. No inter-domain hydrophobic interactions or H-bonding was detected. However, a number of charged residues were found in close proximity between the domains, indicating that electrostatic interaction may be the key factor for the orientation of the two domains. This is the first report of a 3D structure for any MSP. In addition, structural comparison based on DALI, CATH, and CE methods revealed that porcine MSP has a novel structure with a new fold providing valuable information for future structural studies on other MSPs and for understanding their biological functions.

L7

1) The Unique Structures of Nucleic Acid Molecules Adopting Sheared GA Base Pairs, 2) Structural Genomics Studies of *Xanthomonas campestris* pv. *campestris*

Shan-Ho Chou

Institute of Biochemistry, National Chung-Hsing University, Taichung, 40227, Taiwan, ROC

Abstract: 1) In the past decade, we have used high-resolution NMR technique to study unusual DNA structures and found some unique recurring structural motifs associated with sheared base pairs. Such motifs therefore represent stable structural elements that may be of general importance. Extensive studies of such motifs allows us to make some generalization concerning nuclei acid stability: 1) Cross-strand base/base stacking occurs in tandem sheared base pairs; 2) Interdigitated base/base stacking occurs when they are enclosed by sheared base pairs; 3) Base/deoxyribose stacking happen in the single-residue GNA, ANA, ANC, and GNC loops. Thus except the canonical Watson-Crick GC and AT base pairing and intra-strand base-base stacking, many other unique base pairing and stacking modes are available to enlarge the repertoire of DNA structures.

2) The flood of sequence information available from the various genome projects coupled with the recent advances in molecular and structural biology has led to the concept of structural genomics on a genome-wide scale. Determination of protein three-dimensional structures is crucial for understanding their biological functions. *Xanthomonas campestris* is a gram-negative bacterium that is phytopathogenic to cruciferous plants and causes worldwide agricultural loss. However, it also produces exopolysaccharide (xanthan) that is of great industrial importance. Owing to its immense economic impact, we have initiated a large-scale program to determine and characterize the protein structures and functions of *Xanthomonas campestris* using high-field 800 MHz and 600 MHz NMR.

This pathogen genome is first sequenced and its genetic content analyzed by the bioinformatics group. The genes of interests are amplified by PCR method and engineered to P_cold or His-tag vector or vectors containing GST, MBP, or THX fusion gene segment for protein expression in high yields. The desired proteins are purified for NMR studies in one step with or without cleavage of the fusion partners.

The 2D and 3D homo- or heteronuclear NMR spectra were collected by Varian Unity Inova 800 and 600 MHz spectrometers, processed by NMRPipe/NMRDraw programs, and analyzed/assigned using Sparky program. The protein backbone H^N , N, CA, and CB atoms were sequentially assigned

using 2D ^{15}N -HSQC, 3D triple-resonance HNCACB, CBCA(CO)NH, HNCO, and HN(CA)CO spectra. The side chain atoms were assigned using 3D TOCSY-HSQC, HCCH-COSY, HCCH-TOCSY, H(CCCO)NH, and (H)C(CCO)NH spectra. The methyl groups of Val and Leu were stereospecifically assigned based on the relative signs of cross-peaks observed in the CT ^{13}C - ^1H HSQC spectra of $u\text{-}^{15}\text{N}$, 10% ^{13}C -enriched samples. The protein secondary structures were determined by CSI program and the backbone torsion angles Ψ and θ calculated by TALOS program. All these constraints, along with the NOE constraints determined from the 3D-NOESY- ^{15}N -HSQC and NOESY- ^{13}C -HSQC spectra, were served as inputs for CYANA program to calculate the final protein structures.

Through the above-mentioned approaches, over 300 genes have been constructed in high-yield expression vectors, with more than thirty of the gene products exhibiting well-resolved 2D ^1H - ^{15}N HSQC spectra suitable for further structural studies. The recent progress of this project will be reported.

- 1) Chou, S.-H., Chin, K.-H. and Wang, A.H.-J. (2003) Unusual DNA duplex and hairpin motifs. *Nucl. Acids. Res.*, **31**, 2461-2474. (review article)
- 2) Chin, K.-H., Lin, F.-Y., Hu, Y.-C., Sze, K.H., Lyu, P.-J. and Chou, S.-H. (2005) Solution structure of the XC975 from a plant pathogen *Xanthomonas campestris* pv. *campestris*: A bacterial BofA-like protein. *J. Biomol. NMR*, in press.
- 3) Chin, K.-H., Lin, J.-H., Yang, C.-Y., Tu, J.-L., Lyu, P.-J. and Chou, S.-H. (2005) ^1H , ^{15}N , and ^{13}C resonance assignments of a natively unfolded protein XC4149 from the plant pathogen *Xanthomonas campestris* pv. *campestris*. *J. Biomol. NMR*, submitted.
- 4) Chin, K.-H., Zhu, C.-L., Tu, J.-L., Lyu, P.-J. and Chou, S.-H. (2005) Resonance assignments of a polyketide synthesis protein XC5357 from the plant pathogen *Xanthomonas campestris* pv. *campestris*. *J. Biomol. NMR*, submitted
- 5) Chin, K.-H., Yang, C.-Y., Jhe-Le Tu, Tu, J.-L., Lyu, P.-C. and Chou, S.-H. (2005) ^1H , ^{15}N , and ^{13}C resonance assignments of a new member of alkyl hydroperoxide peroxidase XC2714 from the plant pathogen *Xanthomonas campestris* pv. *campestris*. *J. Biomol. NMR*, submitted.

L8

Mutational effect on the β -amyloid peptide discordant helix

Chi-jen Lo^{1,2}, Chin-Ching Wang^{1,2}, Yi-chen Chen³, Hsien-bin Huang⁴, and **Ta-Hsien Lin**^{1,2,5}

¹*Institute of Biochemistry and* ²*Structural Biology Program, National Yang Ming University;*

³*Institute of Medical Science, Tzu Chi University;* ⁴*Institute of Molecular Biology, National Chung Cheng University;* ⁵*Department of Medical Research and Education, Taipei Veterans General Hospital*

Abstract: Alzheimer's disease (AD) a chronic, neurodegenerative disorder which is characterized by progressive dementia beginning in middle to late life with symptoms including loss of cognitive ability, impairment of memory and language, severe behavioral abnormalities, and personality changes. One of the main histopathological hallmarks of AD is the senile plaques within the cerebral cortex. The primary component of senile plaques is a 39-42 residue peptide, β -amyloid peptide¹ ($A\beta$), which is derived from proteolysis of a membrane-spanning glycoprotein known as β -amyloid precursor protein². Many studies have suggested that $A\beta$ has neurotoxic properties in the aggregated state. According to the amyloid cascade hypothesis³, $A\beta$ aggregates are the primary cause of AD. Aggregation of $A\beta$ into fibril is a complex process. A nucleation-dependent polymerization model has been proposed to describe the mechanism of $A\beta$ fibril formation⁴. Recently, Kallberg *et al.* proposed that α -helix/ β -strand-discordant stretches are associated with amyloid fibril formation⁵. For $A\beta$, the predicted discordant region is located between amino acids 15 and 23 (Q₁₅KLVFFAED₂₃). It has also been demonstrated that mutations within this region can abolish α/β -discordance and reduce fibril formation⁵⁻⁷. *In vitro* study of familial early-onset AD case⁸ has found that the Arctic mutation (E22G), a pathogenic AD mutation within the $A\beta$ sequence, had a higher propensity to form soluble $A\beta$ fibril intermediates, $A\beta$ protofibrils, than wild-type $A\beta$, suggesting an alternative pathogenic mechanism for AD. The Arctic mutation can accelerate the formation of protofibrils, however the molecular mechanism is still not entirely understood. The Arctic mutation is located within the α/β -discordant region, suggesting the possibility that it may alter the tendency of α -helix/ β -strand conversions. We report here that the pathogenic Alzheimer's disease mutation, Arctic mutation (E22G), disrupt the α -helicity of $A\beta$ discordant region, suggesting that $A\beta$ with Arctic mutation is more prone to undergo α -helix/ β -strand conversions than wild-type $A\beta$.

Reference

1. Glenner, G.C. & Wong, C.W. *Biochem. Biophys. Res. Commun.* 120, 885-890 (1984).
2. Goldgaber, D., Lerman, J.I., McBride, O.W., Saffioti, U. & Gajdusek, D.C. *Science* 235, 877-880 (1987).
3. Selkoe, D.J. *Physiol. Rev.* 81, 741-765 (2001).
4. Lomakin, A., Teplow, D.B., Kirschner, D.A. & Benedek, G.B. *Proc. Natl. Acad. Sci. U.S.A.* 94, 7942-7947 (1997).
5. Kallberg, Y., Gustafsson, M., Persson, B., Thyberg, J. & Johansson, J. *J. Biol. Chem.* 276, 12945-12950 (2001).
6. Tjernberg, L.O., Näslund, J., Lindqvist, F., Johansson, J., Karlström, A.R., Thyberg, J., Terenius, L. & Nordstedt, C. *J. Biol. Chem.* 271, 8545-8548 (1996).
7. Päiviö, A., Nordling, E., Kallberg, Y., Thyberg, J. & Johansson, J. *Protein Sci.* 13, 1251-1259 (2004).
8. Nilsberth, C. *et al. Nat. Neurosci.* 4, 887-893 (2001).

L9

Solution Structure of a Plant Defensin VrD1 from Mung bean: A Possible Mechanism for Insecticidal Activity Against Bruchid

Yaw-Jen Liu¹, Chao-Sheng Cheng¹, Ming-Pin Hsu³, Ching-San Chen^{3, 4*} and Ping-Chiang Lyu^{1, 2*}

¹*Department of Life Sciences, National Tsing Hua University, Hsinchu, Taiwan*

²*Institute of Bioinformatics and Structural Biology, National Tsing Hua University, Hsinchu, Taiwan*

³*Institute of Botany, Academia Sinica, Nankang, Taipei, Taiwan*

⁴*Institute of Microbiology and Biochemistry, National Taiwan University, Taipei, Taiwan*

Abstract: *Vigna radiate* plant defensin 1 (VrD1), isolated from mung bean (*Vigna radiata*), is the first reported plant defensin exhibiting *in vitro* insecticidal activity against bruchid. We reported here the NMR solution structure and its implication in insecticidal activity of VrD1. The root-mean-square deviation values are 0.51 ± 0.35 Å and 1.23 ± 0.29 Å for backbone and all heavy atoms, respectively. The structure of VrD1 consists of a 3_{10} helix, an α -helix, and a triple-stranded anti-parallel β -sheet stabilized by four disulfide bonds, forming a typical cysteine-stabilized $\alpha\beta$ motif. Among the known structured plant defensins, VrD1 is the first defensin with an additional 3_{10} helix. The replacement of the highly conserved glutamate by arginine at residue 26 in VrD1 may induce a shift in the orientation of Trp¹⁰ and form the additional 3_{10} helix. Both sequence and structure comparisons reveal a high degree of similarity between VrD1 and insect α -amylase inhibitors. Since α -amylase is a digestive enzyme in the insect gut and plays an essential role in the digestion of plant starch, computational analyses were used to test the possibility of interactions between VrD1 and insect α -amylase. The expression of the common bean α -amylase inhibitor 1 in transgenic pea showed complete resistance against bruchid, thus this inhibition of protease is of great potential biotechnological interest. Our docking results also provide useful interaction information that may improve the insecticidal activity of VrD1.

L10

Heparin-mediated cellular internalization of Hepatoma-derived growth factor: Role of the conserved N-terminal HATH domain

Shih-Che Sue

Institute of Biomedical Sciences, Academia Sinica, Nankang, Taipei, Taiwan, R.O.C.

Abstract: Human hepatoma-derived growth factor (hHDGF) is a heparin-binding protein that was implicated in tumorigenesis, vascular development, cell proliferation and transcriptional activation. NMR solution structure of hHDGF is reported here that it comprises an ordered N-terminal domain (HATH domain, ~ 100 a.a.) and a highly disordered C-terminal domain (~140 a. a.). The N-terminal HATH domain is proved to be responsible for specifically interacting with heparin that the disordered C-terminal region exhibits no heparin-binding ability but shows transformation activity to enhance cell saturation density and growth rate. Meanwhile we demonstrate that HATH domain along is capable to delivery fluorescence proteins, DsRED and GFP, into cytoplasm and nuclear in the different cell lines. HATH domain shows the ability to serve as a potential carrier for aiding protein internalization. The process is further examined in a heparin-expression-defective CHO K1 cell line to determine the importance of heparin. Noticeably, the defective expression of heparin in cell surface completely abolishes the internalization process of hHDGF, implying the critical role of binding to heparin in the case of hHDGF. These results prove that the N-terminal HATH region promotes the entry of protein into the cell through binding to heparin molecule, while the C-terminal region may be responsible for regulation of its activity Furthermore, the N-terminal HATH domain is identified to have monomeric and dimeric formations in physiologic condition, that dimeric form shows strong heparin-binding affinity of $K_d \sim 10$ nM, however monomer loses such strong binding-behavior. Biochemical studies are performed to characterize the heparin binding length and sequence for dimeric HATH domain. In final, a hypothetical mechanism is addressed here to allow us to prospect the correlation between dimeric property and heparin-mediated cell entry.

L11

Biophysical Studies on Amyloid Fibrillization of Human Pancreatitis-Associated Protein (hPAP)

Yuan-Chao Lou¹, Meng-Ru Ho^{1,2}, Wen-Chang Lin¹, and Chinpan Chen¹

¹*Institute of Biomedical Sciences, Academia Sinica, Taipei, Taiwan, ROC;* ²*Institute of Bioinformatics and Structural Biology, College of Life Science, National Tsing Hua University, Hsinchu, Taiwan, ROC*

Abstract: Pancreatitis-associated protein (PAP) was first found in pancreatic juice during the acute phase of pancreatitis. It is a 16-kDa secretory protein and was found in many vertebrates. All PAP proteins share a common C-type animal lectin motif in the C-terminus. Human PAP was detected in several human cancer tissues such as liver, colon and stomach and in developing and regenerating motor neurons. Several biological functions have been proposed for PAP, but the real one remains elusive. Recently, PAP was strongly suggested to be an anti-inflammatory factor, and was found to be involved in the very early stages of Alzheimer's disease (AD). It was suggested that PAP together with another anti-inflammatory protein, PSP, may trigger or accelerate the aggregation of A β and Tau (the major protein precipitation found in AD) to form amyloid fibrils. For many of these amyloid diseases, the major protein component of the fibrillar deposit has been identified. They are different in amino acid sequences and native folds, but all can form misfolded, insoluble amyloid fibrils with common 'cross- β ' structural elements. In our studies, we found that hPAP tends to form amyloid fibrils at neutral pH, while remains soluble at acidic condition. To gain insight into the mechanism of amyloid fibrillization of hPAP, we applied NMR as well as other biophysical techniques, like circular dichroism (CD), FT-IR, analytical ultracentrifugation, and electron microscopy, to carry out biophysical studies on hPAP. Combining all the structural and biophysical studies, we hope that the process of amyloid fibrillization of human pancreatitis-associated protein could be realized.

L12

Solution Structure of the Hypothetical Protein HP0495 from *Helicobacter Pylori*

Ya-Ping Tsao, Zheng-Zhong Huang, Wei-Ting Li, Chui-Lin Chiu, Jya-Wei Cheng

Institute of Biotechnology and Department of Life Science, National Tsing Hua University, Hsinchu, 300 Taiwan

Abstract: *Helicobacter pylori* known as gastric pathogenic bacteria is able to cause digestive illnesses including gastritis and peptic ulcer disease. Its genome has been completely sequenced. The next step of genomic studies after the yielding of the complete genome sequence of the species is to identify both cellular and molecular function of each gene in the genome.

In our present studies, thirty of the *H. pylori* genes are chosen for structural studies by CD and NMR with isotope tagged proteins. Structural and functional studies of HP0495, a hypothetical protein, HP1492, nitrogen fixation protein, HP0222, an acid induced protein, and HP1442, a carbon storage regulator protein, have been carried out using CD and NMR.

The HP0495 gene of *H. pylori* encodes a hypothetical protein of 86 amino acid residues with a molecular weight of 10,193 Da and a calculated isoelectric point of 8.7. HP0495 has no identifiable sequence homology to any well-characterized proteins. However, protein-protein interaction map of *H. pylori* showed that HP0495 interacts strongly with HP1205. HP1205 is strongly similar to translation elongation factor EF-Tu, thus, HP0495 may be involved in the protein synthesis. Solution structure studies of HP0495 reveals that the overall fold of this protein consists of three beta-strands and two alpha-helices. Knowledge of the structure of HP0495 will help the functional studies of its role in human diseases.

致謝:

磊葳科技股份有限公司

分子視算股份有限公司

大陳生物科技股份有限公司

化譜有限公司